Agricultural and Forest Meteorology 151 (2011) 204–214

Contents lists available at ScienceDirect

Agricultural and Forest Meteorology

journal homepage: www.elsevier.com/locate/agrformet

Field characterization of olive (*Olea europaea* L.) tree crown architecture using terrestrial laser scanning data

Inian Moorthy[a,*], John R. Miller[a,b], Jose Antonio Jimenez Berni[c], Pablo Zarco-Tejada[c], Baoxin Hu[b], Jing Chen[d]

[a] Centre for Research in Earth and Space Science (CRESS), Petrie Science and Engineering Building, York University, 4700 Keele Street, Toronto, Ontario M3J 1P3, Canada
[b] Department of Earth and Space Science and Engineering, Petrie Science and Engineering Building, York University, Toronto, Ontario, Canada
[c] Instituto de Agricultura Sostenible (IAS), Consejo de Superior de Investigaciones Cientificas (CSIC), Cordoba, Spain
[d] Department of Geography and Planning, University of Toronto, St. George Campus, Toronto, Ontario, Canada

ARTICLE INFO

Article history:
Received 29 March 2010
Received in revised form 15 October 2010
Accepted 18 October 2010

Keywords:
Laser scanning
ILRIS-3D
Biophysical parameters
Olea europaea L.

ABSTRACT

Since the introduction of Terrestrial Laser Scanning (TLS) instruments, there now exists a means of rapidly digitizing intricate structural details of vegetation canopies using Light Detection and Ranging (LiDAR) technology. In this investigation, Intelligent Laser Ranging and Imaging System (ILRIS-3D) data was acquired of individual tree crowns at olive (*Olea europaea* L.) plantations in Córdoba, Spain. In addition to conventional tripod-mounted ILRIS-3D scans, the unit was mounted on a platform (12 m above ground) to provide nadir (top–down) observations of the olive crowns. 24 structurally variable olive trees were selected for in-depth analysis. From the observed 3D laser pulse returns, quantitative retrievals of tree crown structure and foliage assemblage were obtained. Robust methodologies were developed to characterize diagnostic architectural parameters, such as tree height ($r^2 = 0.97$, rmse = 0.21 m), crown width ($r^2 = 0.97$, rmse = 0.13 m), crown height ($r^2 = 0.86$, rmse = 0.14 m), crown volume ($r^2 = 0.99$, rmse = 2.6 m^3), and Plant Area Index (PAI) ($r^2 = 0.76$, rmse = 0.26 m^2/m^2). With the development of such LiDAR-based methodologies to describe vegetation architecture, the forestry, agriculture, and remote sensing communities are now faced with the possibility of replacing current labour-intensive inventory practices with, modern TLS systems. This research demonstrates that TLS systems can potentially be the new observational tool and benchmark for precise characterization of vegetation architecture for improved agricultural monitoring and management.

1. Introduction

Current methods for remote detection of plant physiology are inhibited by limitations in the explicit information about vegetation structure. The spatial architecture of plant material, within natural and plantation-like environments, plays a pivotal role in controlling functional activities like photosynthesis and evapotranspiration. As such, recent advancements have addressed this challenge using Light Detection And Ranging (LiDAR), an active remote sensing technology. Traditional remote sensing approaches "indirectly" determine plant architecture and physiology using data from passive optical imaging sensors. These methods rely on variability in vegetation spectral responses from the visible and near-infrared spectral regions. Widely accepted algorithms such as the Normalized Difference Vegetation Index (NDVI) have been empirically correlated to structural parameters such as canopy-level Leaf Area Index (LAI). Unlike passive optical imaging sensors, which are only capable of providing detailed measurements of vertically integrated horizontal distributions in vegetation canopies, LiDAR systems can yield highly specific information in both the horizontal and vertical (depth) dimensions (Lim et al., 2003). LiDAR-based instruments from airborne and ground-level platforms provide a "direct" means of measuring crown-level architecture, previously unattainable using passive remote sensing imagery. LiDAR units employ the Time-Of-Flight (TOF) principle or phase-based differences to measure the distances of objects based on the time interval between laser pulse exitance and return, upon backscattering from an object. The acquired LiDAR point cloud of returns yield a 3D digital representation of the vegetation environment in which each point is characterized by an *XYZ* coordinate. The challenge within the remote sensing community is to now develop robust methodologies that utilize such highly specific 3D point cloud data to directly retrieve canopy structural attributes thereby addressing the current scientific need for precise *in situ* measures of vegetation biophysical parameters (Maas et al., 2008). Applications of LiDAR systems from airborne platforms have characterized tree

* Corresponding author. Tel.: +1 416 736 2100x40218.
E-mail address: moorthy@eol.esse.yorku.ca (I. Moorthy).

0168-1923/$ – see front matter © 2010 Elsevier B.V. All rights reserved.
doi:10.1016/j.agrformet.2010.10.005

crown structure from both discrete return recordings (Coops et al., 2004; Donoghue et al., 2007; Jang et al., 2008; Lefsky et al., 1999; Thomas et al., 2006) and waveform recordings (Harding et al., 2001; Lefsky et al., 2002; Means et al., 1999; Patenaude et al., 2004). The backscattered laser pulses from Airborne Laser Scanning (ALS) systems have been used to extract various dimensional parameters, such as tree height (Andersen et al., 2006; Morsdorf et al., 2004; Hopkinson, 2007; Yu et al., 2004), crown dimension (Means et al., 2000; Popescu and Zhao, 2008), and crown volume (Hinsley et al., 2002; Riaño et al., 2004). Retrievals from discrete airborne LiDAR systems have the advantage of capturing information over a large area, but are constrained by their laser pulse return density (pts/m^2). Multi-echo reading capabilities of ALS platforms produce somewhere between 3 and 20 backscattered pulses/m^2. Often this level of detail is insufficient to provide a detailed profile, especially in the vertical axis, of the tree crown that is required for precision 3D radiative transfer modeling. The ability to acquire laser pulse echoes from the bottom part of vegetation canopies is confounded by the ALS system properties (i.e. laser footprint size, recording frequency, etc.) as well as the organization of the crown elements themselves (i.e. closed vs. open canopies). As such, it is logical to introduce the use of LiDAR systems at ground level for much higher resolution laser pulse densities and thereby enabling detailed specification of canopy organization and individual tree crown characterization.

Ground-level, Terrestrial Laser Scanning (TLS), conventionally used for mining, urban planning and surveying applications, are now used to rapidly measure intricate structural details of vegetation canopies (Côte et al., 2009; Jupp et al., 2009; Lichti et al., 2002; Omasa et al., 2007; Rosell et al., 2009; Strahler et al., 2008). The unique perspective of such portable TLS systems allows the characterization of the vertical distribution of vegetation structure (Radtke and Bolstad, 2001), potentially replacing current labour-intensive, and manual field inventory practices. By mounting a laser ranging system on a pan/tilt platform Lovell et al. (2003) cross-validated laser-derived Leaf Area Index (LAI) estimates to those obtained by hemispherical photography to within 8% for mixed evergreen canopies in Australia. More recently, TLS data has been used to estimate other photosynthetically significant parameters, such as plant area densities (Takeda et al., 2008; Hosoi and Omasa, 2009), and the ratios of woody to total plant areas (Clawges et al., 2007). Additional research that focused on the measurement and segmentation of tree stem diameters and branching structures has also been conducted (Henning and Radtke, 2006; Hopkinson et al., 2004; Thies et al., 2004). Although the delineation of stem diameters is tree specific, the previous retrievals of LAI are spatially integrated for the entire canopy. Appropriate ground LiDAR data acquisitions also offer the potential of calculating LAI at the individual crown level provided that 3D point cloud data can be acquired for isolated crowns. Accordingly, this research is focused on estimating critical biophysical parameters that describe tree crown dimensional properties, as well as the foliar assemblage characteristics, using TLS data for individual tree crowns within an organized plantation.

2. Materials and methods

2.1. Field study area

The experiments were conducted at four olive (*Olea europaea* L.) plantations near the Institute for Sustainable Agriculture (IAS) in Córdoba, Spain (37.85° N; 4.8° W) (Fig. 1). The area is defined by typical Mediterranean climate, with an average annual rainfall of 600 mm, primarily concentrated outside the 4-month summer drought period (Moriana and Orgaz, 2003; Pastor et al., 2007). The average temperatures during the mild Autumn–Spring months are approximately 14–21 °C, and decrease to about 5 °C in the coldest month, January. The soil in the region is a Typic Xerofluvent of alluvial sandy loam, and low in organic matter. Prior to field data acquisition a scouting mission was conducted to pre-select 24 sample trees from four orchards with tree spacing of 6 m × 6 m (277 olive trees ha^{-1}), or 7 m × 7 m (204 olive trees ha^{-1}). The selected trees were representative of the structure and age conditions exhibited for the plantations in the region.

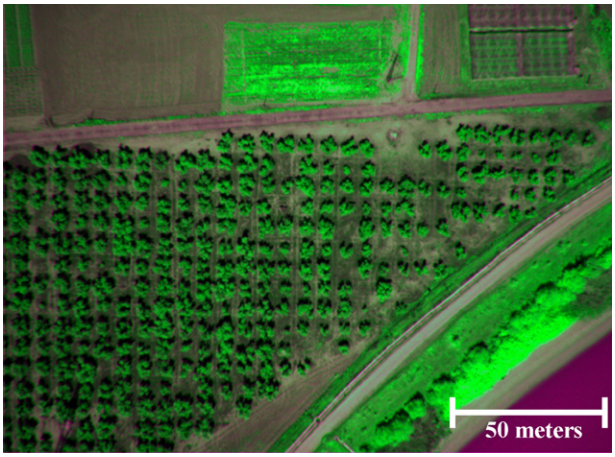

Fig. 1. Airborne image (550 nm-red, 800 nm-green, 670 nm-blue) of olive (*Olea europaea* L.) discontinuous canopies in Córdoba, Spain. 24 trees were selected from four olive plantations for detailed structural characterization using the ILRIS-3D (for interpretation of the references to color in this figure legend, the reader is referred to the web version of the article).

2.2. Laser scanning of olive trees

Ground-based laser scanning data of the olive trees were acquired using the Intelligent Laser Ranging and Imaging System (ILRIS-3D) developed by Optech Incorporated, Toronto, Canada. The ILRIS-3D is a robustly designed, camera-viewing (40° × 40° FOV), long-range scanner (3–1000 m) that operates at a scanning rate of 1500 laser pulses per second. The minimum spot spacing between laser pulses is 0.026 mm × R, where R is the range distance in meters. The laser pulse diameter is 12.7 mm at exitance and degrades at a rate of 0.17 × R. The system has a beam divergence of 0.00974° (0.17 mrad) and a minimum spot step (X- and Y-axis) of 0.00115° (0.02 mrad). A high-speed counter within the ILRIS-3D measures the time of flight from the start of a laser pulse to the return of that pulse. Based on that time measurement, the distance or range of a reflecting object is derived. This TOF approach yields detailed coordinates (XYZ) of each detected object with the scanned area. In February, 2007 the ILRIS-3D was deployed to the field study area in Córdoba, Spain for precision measurements of olive tree crown architecture, from conventional ground tripod-mounted as well as nadir perspectives.

2.2.1. Tripod-mounted ILRIS-3D data collection

For the horizontal perspectives of the olive trees, the ILRIS-3D unit was mounted on a tripod and positioned so that there was a clear line of sight between the scanner and the target tree. Specific locations were chosen to minimize the influence of obstructing elements, mainly branches from neighboring trees. Such obstructing elements can lead to improper estimation of crown attributes, due to the shadowing effect that they impose on the selected individual tree. In addition, due to the intrinsic long-range scanning properties of the ILRIS-3D, the system had to be positioned at a distance greater than 3 m from the tree. First-return laser XYZ point clouds were acquired for all 24 trees with a resolution of 5 mm at 10 m. If

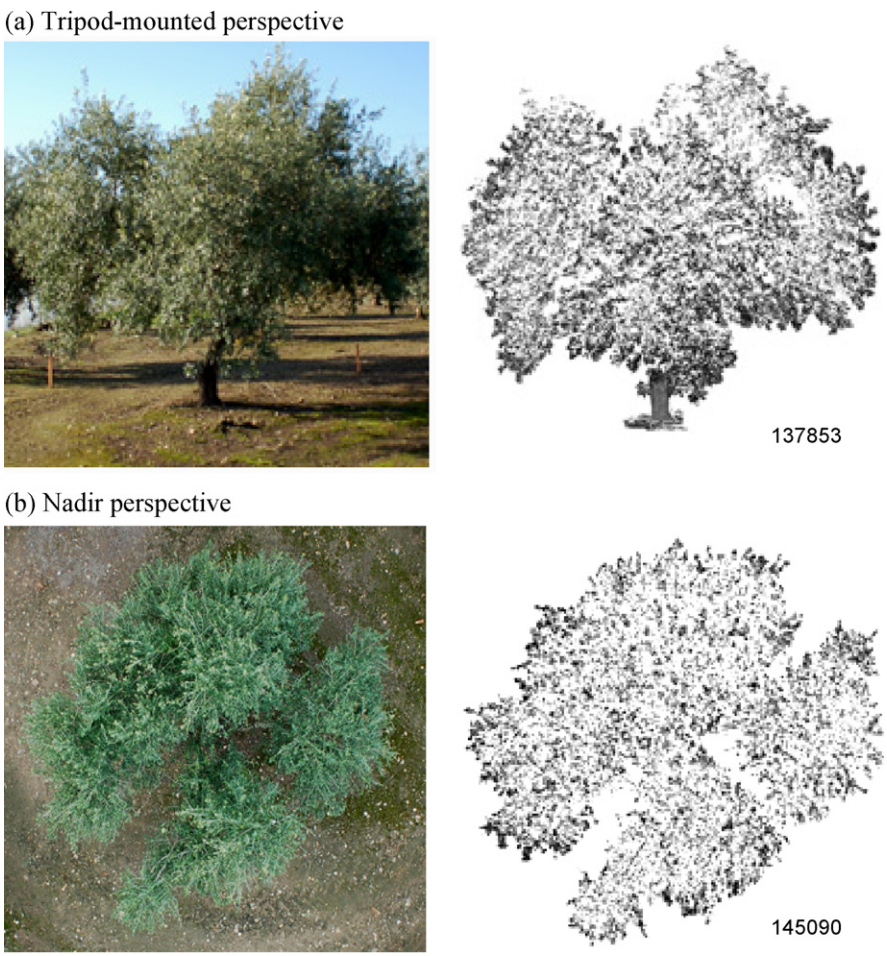

Fig. 2. An example of an ILRIS-3D point cloud of an olive tree from (a) tripod-mounted and (b) nadir perspective. Such measurements yield over 100,000 laser pulse returns per individual tree crown.

the tree spacing of the orchard was large enough, the same tree was scanned from two diametrically opposing viewpoints. Whenever possible, the distance between the tree and the scanner for opposing scans was kept consistent. However, due to the geometry and organization of the plantations, acquiring multiple tripod-mounted perspectives was not always feasible. Opposing perspective scans were acquired for 17 of the 24 sample olive trees. Prior to scan acquisition, various targets, in the form of wooden stakes, were placed both in the foreground and background, surrounding the tree. The positional locations of the stakes were acquired with a total station using standard survey methodology. These stakes were used as ground control points to co-register the *XYZ* point clouds from multiple viewpoints to generate a more complete 3D representation of the crown. TLS observations of the olive trees in the study area yield *XYZ* point clouds with greater than 100,000 individual return laser pulses per tree, thereby describing in detail the wide range of structural conditions with the olive orchards (Fig. 2a).

2.2.2. Nadir ILRIS-3D data collection

The nadir-perspective data was obtained by mounting the ILRIS-3D sensor onto the platform of a mobile cherry picker. The platform was elevated to approximately 10–15 m above the ground, with a minimum distance of 3 m between the sensor and the top of the tree crown. Positioned directly overtop the crown, this approach offers a viewpoint that is similar to an Airborne Laser Scanning (ALS) instrument, but provides a much higher number of laser pulse echoes as a result of the close proximity to the tree crown (Fig. 2b). The density of returned pulses from the TLS system is greater than ALS by 3–4 orders of magnitude. The resolution, or spacing between laser pulses, of the nadir scans was 5 mm at 10 m. All ILRIS-3D data was obtained under calm conditions to limit the noise/errors caused by wind gusts moving the leaves and branches of the crowns.

2.3. Field mensuration data of olive trees

Furthermore, additional ground-level efforts have been made to collect *in situ* measurements of crown structure using traditional methods as well as using the LAI-2000 Plant Canopy Analyzer (PCA). Validated protocols for olive tree structural parameter measurements have been established in previous works by scientists at the IAS (Villalobos et al., 1995). Dimensional properties, namely crown height and crown width, are measured at multiple points within a given olive tree using transects. Each crown is divided into eight sections using four equal-angle spaced transects. Seven points along each transect are selected and, using a ruler, the top and bottom extents of the crown at each position is recorded. This approach effectively yields a low-resolution 3D point cloud that represents the dimensional extents of the olive tree crown. In addition to *in situ* measurements of crown dimensions, the LAI-2000 Plant Canopy Analyzer (PCA) was used to estimate leaf area index at the individual crown level. Diffuse radiation readings above and below the tree crown at five zenith angles were recorded with the PCA. From these readings the gap fraction as a function of plant area density is determined. PCA estimates the surface area of all the phytoelements in the field of view, thus including green and non-green elements. PCA measurements under the influence of direct sunlight

can lead to an underestimation of LAI (Welles and Norman, 1991), due to increased scattering of diffuse radiation beneath the canopy (Villalobos et al., 1995). Accordingly, PCA data was acquired before sunrise or after sunset to limit the confounding effect of direct sunlight. The Plant Area Density (PAD) was calculated using four measurements of the PCA positioned beneath the canopy pointing at the four cardinal directions using the 90° viewing cup. The measured PAD values are then used to calculate LAI based on path lengths for each crown using the protocol from Villalobos et al. (1995). As a result of intensive management practices at the experimental olive plantations near the IAS, some of the selected olive trees were pruned after LiDAR data was obtained and unfortunately before the possibility of field measurements. The pruning process altered the structural properties of some target trees after the time of TLS observations, rendering these trees an ineffective validation data source. As a result, usable mensuration data was only acquired for 11 of the 24 trees originally selected for detailed study. This subset of the complete data source was used to assess/validate the TLS-based retrievals.

2.4. Analysis of LiDAR data for tree crown structure

2.4.1. Defining crown shape primitive

The ILRIS-3D point cloud data was processed using a cross-sectional slicing algorithm that was developed and tested in laboratory trials with an artificial tree (Moorthy et al., 2008). The algorithm separates the *XYZ* laser pulse returns into a user-specified number of cross sections, as a function of distance from the scanner. The flexibility of this approach allows the interrogation of both horizontal and nadir perspectives of the TLS data. Thus for the horizontal perspective, TLS data can be evaluated as a function of distance into the crown and for the nadir viewpoint, the *XYZ* points are evaluated with a top/down approach, where the first slice is the top of the tree crown. There are several previous inventory-based TLS studies that focus on the accurate retrieval of the stem properties, such as diameter-breast-height (DBH) (Henning and Radtke, 2006; Hopkinson et al., 2004; Thies et al., 2004). In this investigation, however, the focus was to estimate the physical dimensions and the spatial distribution of the foliage architecture within the envelope of the crown. Consequently, in the analysis of the horizontal *XYZ* scans, a stem threshold value (i.e. bottom of crown height) was incorporated into the algorithm, thereby excluding all returned laser pulses below that limit. Inclusion of the returns from the trunk, although pertinent to stem attributes, would complicate the extraction of crown shape physical properties, as well as confound the methods of foliage distribution estimation.

In this investigation, the first focus was to estimate the crown physical dimensions of the targeted olive crowns. As such, the ILRIS-3D point cloud of each tree was analyzed using a slicing algorithm, which separated the data into 100 cross-sectional slices. The number of pulse returns that fall within each slice was tabulated. This tabulation along with the total number of pulse reflections from the entire tree are used to calculate the fractional pulse return to profile crown architectural shape and variability. This level of detail and type of analysis illustrates the intra-crown foliage variations at cm-scale resolutions. The flexibility of the slicing algorithm allows the LiDAR point cloud to be analyzed (i.e. sliced) both along and perpendicular to the viewing axis. The returned laser pulses are separated with slices parallel (*XY* plane) to the ground to determine tree height H, and crown width E_x (Fig. 3a and c). The same point cloud can be evaluated with slices perpendicular (*XZ* plane) to the ground to determine the effective crown height dimension E_z (Fig. 3b and d). Tree height H, was estimated using the difference in laser pulse reflection from the top of the crown and the ground. The laser pulse returns and their spatial distribution within are used to generate an irregular polygon outline or convex hull for each individual slice. Using a triangulation approach, the area of the outlined polygon of each slice is calculated (Moorthy et al., 2008). Determination of the number of pulses per slice and the areal coverage of each slice provides a retrieval of the laser pulse return density (pts/m^2), an indicator of within-crown foliage density and distribution. The calculated area is then used to determine the radius of a circle with an area equivalent to the irregular polygon. This radius is a measure of the crown width (E_x) at a specific range distance which can then be profiled for each individual crown (Fig. 3c). This process of delineating the crown dimension is repeated for the other principal axis of the shape primitive by slicing the original point cloud with cross sections that are normal (*XZ* plane) to the ground. The resultant profiles define the crown height (E_z), as a function of distance into the crown, from the first reflected laser pulse to the last for each tree crown (Fig. 3d). From these profiles, the maximum values of E_x and E_z are acquired and used to draw a representative spheroid of the tree crown (Fig. 3e). The derived spheroid is not intended to surround all foliage/branch elements, but rather effectively represent the crown by an equivalent primitive 3D object, based on the laser pulse reflections. The relative proportions of E_x and E_z indicate whether the spheroid is prolate ($E_z > E_x$) or oblate ($E_z < E_x$). Since one of the objectives of the investigation was to compare the retrievals from the horizontal perspective versus the nadir perspective, a similar analysis was needed for the nadir observations. E_x and E_z profiles were calculated with slices along the *XZ* and *YZ* planes, respectively. Maximum E_x and E_z were recorded and subsequently compared with the retrievals from the horizontal viewpoints. The different perspectives produce different occlusion effects, thereby influencing the estimates of the crown physical dimensions. The acquisition of TLS data from both the nadir and tripod-mounted perspectives allows an assessment of the benefits and limitations of such scans for operational monitoring for precision orchard management.

2.4.2. Defining foliage assemblage: PAI and clumping index

Once the crown dimensional properties were extracted, the focus of the analysis shifted to describing the assemblage of foliage material within individual crowns. The scattering elements within the real olive crown can be represented with a few parameters, namely Leaf Area Index (LAI) and clumping index (Ω), within the representative spheroid as defined in Fig. 3. Following the methodology developed in Moorthy et al., 2008, gap fraction (P), or the probability of a pulse being transmitted through the crown without encountering any objects was calculated. In other words, the return of an emitted laser pulse means 0% gap (i.e. encountered an object with sufficient backscattering energy), and lack of return for a given pulse means 100% gap (i.e. insufficient backscattering energy). All points recorded by the ILRIS-3D, both within and outside of the derived crown envelope are used to calculate gap fraction. The pulse return density is integrated for all the cross sections and compared to the theoretical solid object density at the equivalent range distance and area. This methodology uses the spatial distribution of all the detected elements of the complex tree structure to calculate a gap fraction and the simplified representative crown shape primitive. The theoretical backscattered pulse density is controlled by the ranging distance and the user-controlled spatial resolution. These two factors along with the sensor's intrinsic degradation of the resolution (i.e. decay of spot spacing with range) are sufficient variables that can be used to model the maximum possible return density at any given distance from the scanner. Such a laser pulse return model was developed for the ILRIS-3D from laboratory studies (Moorthy et al., 2008) and follows a similar approach for other ground-based laser scanners (Danson et al., 2007). The utilized model includes the assumptions that there are no pulse losses due to environmental factors such as the atmosphere. Infrared light propagation can be attenuated by water vapor, dust particles and

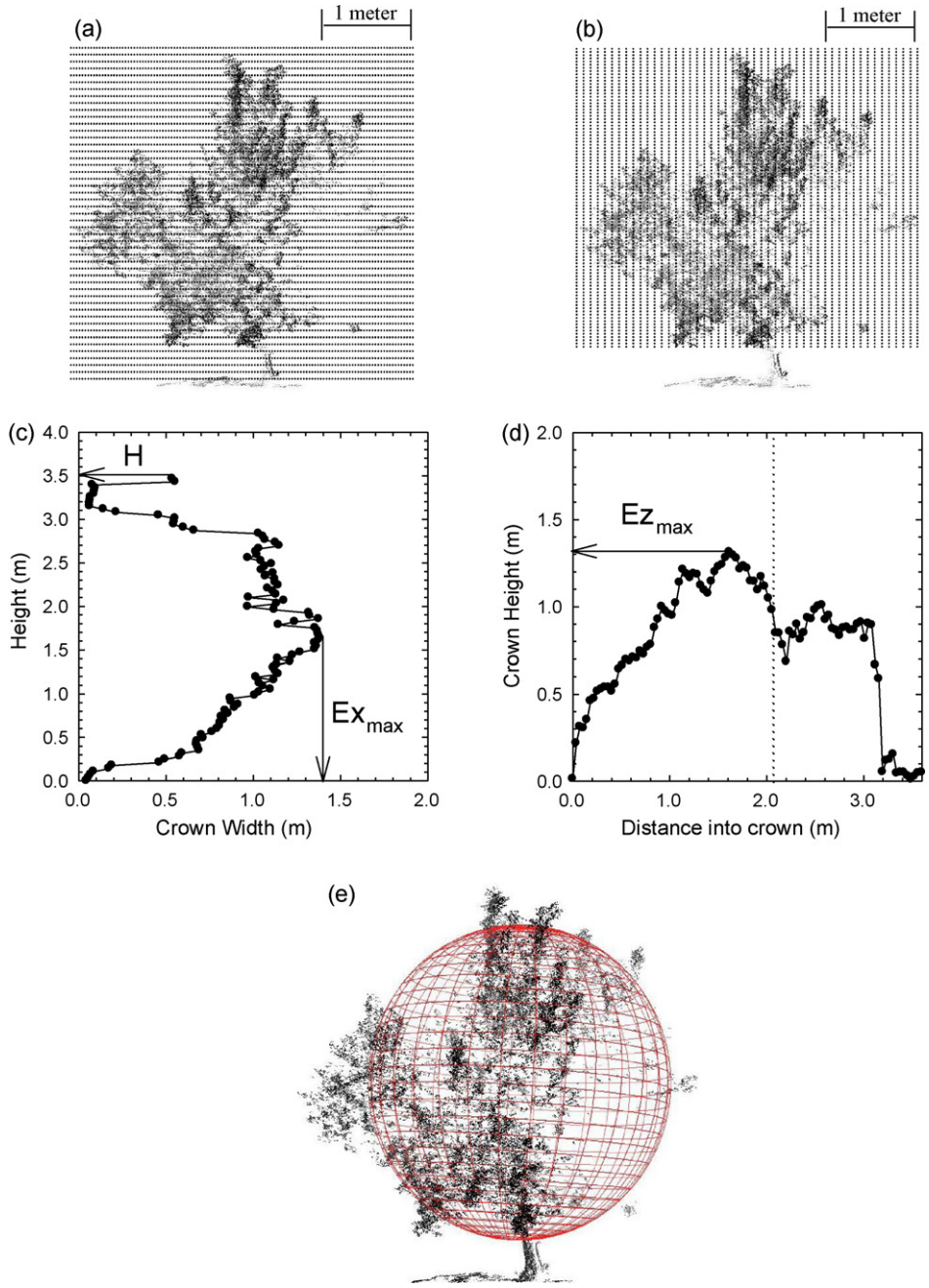

Fig. 3. Methodology for estimating crown extents involves scanning the tripod-mounted scans with (a) a top–down approach, followed by (b) a front-to-back of crown direction. This technique yields specific contours of (c) crown width, E_x, and (d) crown height, E_z, from which maximum values are extracted to define a (e) crown representative spheroid.

smoke thereby reducing detection range and accuracy. However, ILRIS-3D scans were acquired on dry, clear days to minimize this effect. Furthermore, the effects of atmospheric attenuation of the laser beam were negligible due to the relatively short range (<20 m) between the ILRIS-3D unit and the tree. This investigation employs an approach where indirect estimates of leaf area index (LAI) are determined through direct measurements of gap fraction (Moorthy et al., 2008). The calculated gap fraction (P) for each crown can then be inverted to retrieve LAI values using equation (1):

$$P(\theta) = e^{-G(\theta)\Omega \mathrm{LAI}/\cos(\theta)}, \quad (1)$$

where $G(\theta)$ = G function (mean projection of unit foliage area) and Ω = clumping index (non-randomness factor).

The geometry function $G(\theta)$ is used to represent the mean projection of a unit foliage area in the direction θ and is characterized by the Leaf Angle Distribution (LAD). LAD values were calculated based on manual experiments conducted at the Institute of Sustainable Agriculture from olive crowns at the selected study sites (Suarez et al., 2009). The measured distributions of leaf angles within typical olive tree crowns yielded G function values of 0.70 and 0.36 for nadir and horizontal view directions, which were used in equation (1). With an empirical measurement of $G(\theta)$ and gap fraction P determined from the laser point cloud, we can invert equation (1) to retrieve LAI provided the clumping index (Ω) is known. In this investigation leaf and woody material were not distinguished from one another in the LiDAR point clouds. As such, the term Plant Area Index (PAI) rather than LAI is a more appropriate label

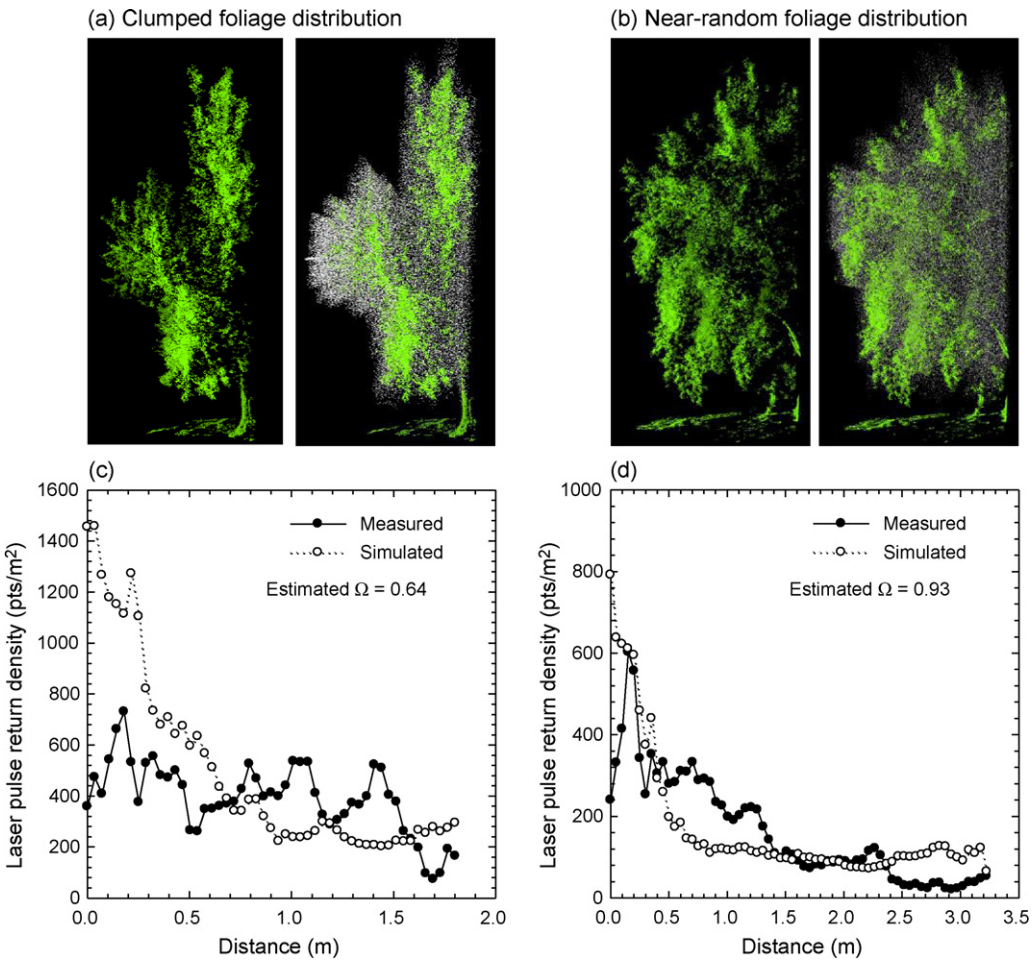

Fig. 4. Measured *XYZ* ILRIS-3D point cloud (green points) superimposed with redistributed random (white points) for (a) highly clumped and (b) near random olive crown. Olive crown with a clumped architecture shows a pulse density profile (c) that is significantly different than the simulated exponential decay of a random crown. Another crown with near random foliage distribution shows similar profiles (d) for measured and simulated cases, illustrating and confirming a clumping index near unity (for interpretation of the references to color in this figure legend, the reader is referred to the web version of the article).

for the measure of the foliage assemblage. Separation of leaf and woody material using the ILRIS-3D remains a challenging issue that requires further calibration and validation of the currently radiometrically invalidated LiDAR measured radiances. Nonetheless, PAI is directly related to LAI, which is a critical determinant of forest status. Such measures of foliage assemblage are usually spatially integrated across the canopy rather than considered on an individual crown basis. However, the high density of *XYZ* coordinates for individual trees allowed the calculation of PAI at a crown-specific level, a measure unique to this study. Such an approach can now be used to provide crown-level management of structural conditions in plantations and orchards for precision agricultural needs.

Furthermore, the *XYZ* point cloud dataset was used to calculate the clumping index, or degree of randomness of the crown structure. The clumping index (Ω), is a correction factor of the PAI calculations that accounts for the spatial organization of foliar elements, and its deviation from a random arrangement. Since clumping index is evaluated as a deviation from randomness, simulations were conducted to generate randomly distributed elements within the crown. The developed methodology utilizes the cumulative number of measured laser pulses for the tree and re-distributes them within the boundary space as defined by the limits of the measured crown dimensions. The boundary space for the random crown has the same individual slice areas as the clumped tree crown. These simulated crowns were then analyzed with the slicing algorithm and it was observed that the laser average pulse return densities of the simulated random crowns have an exponential decay as a function of distance, which can be theoretically described using Beer's law of extinction (Moorthy, 2009). Comparing the measured pulse densities of real clumped crowns versus the simulated densities of random foliage distribution crowns yields clues to the degree of clumping for the olive crowns, which in turn will help understand radiation interception within olive plantations (Fig. 4). Crowns with randomly distributed elements within the crown volume exhibit an exponential decrease in backscattered pulse density as a function of distance into the crown. Clumped crowns are distinguished by more variable density profiles deviating from the exponential trend (Fig. 4c). Comparing the ratio of the gap fraction between the actual measured crown and the randomly organized simulated crown is an indicator of the clumping index (Chen and Cihlar, 1995). The clumping index is calculated by equation (2):

$$\Omega = \frac{\ln[P_{\mathrm{m}}(\theta)]}{\ln[P_{\mathrm{o}}(\theta)]}, \tag{2}$$

where $P_{\mathrm{m}}(\theta)$ = measured gap fraction and $P_{\mathrm{o}}(\theta)$ = imaginary gap fraction of randomly organized crown.

This index is obtained for all the olive crowns, and used as a correction factor when comparing the ILRIS-3D-derived PAI values with the ground measurements.

Table 1
ILRIS-3D retrievals for tree height and crown dimensions for 24 olive trees.

		Minimum	Maximum	Mean	Standard deviation
Tree height	Nadir	1.88	5.81	4.14	0.96
	Horizontal	1.89	5.46	3.93	0.88
Crown width	Nadir	0.76	3.02	1.93	0.67
	Horizontal	0.68	2.58	1.72	0.55
Crown height	Nadir	0.61	2.28	1.56	0.42
	Horizontal	0.58	2.72	1.71	0.56

3. Results and discussion

3.1. Olive crown dimensional properties

Tree height (H), crown width (E_x), and crown height (E_z) were the primary tree structure parameters that were extracted from the TLS point clouds. Since the investigation was able to acquire data from multiple perspectives, it was feasible to estimate these crown dimensions from both the nadir and the horizontal observations for inter-comparison. The ILRIS-3D point clouds were first processed to generate profiles of pulse retrievals for individual crowns showing the fraction of returned laser pulses as a function of distance from the TLS unit. From the laser pulse return profiles, tree heights, crown widths and crown heights were determined to illustrate the variability of the selected crowns in the plantations (Table 1). The estimates from the nadir perspectives are similar to the horizontal perspectives. The mean values for tree height, crown width and crown height from the nadir observations were 4.14 m, 1.93 m and 1.56 m, respectively. From the horizontal measurements the mean estimates were 3.93 m, 1.72 m, and 1.71 m, respectively. Such initial agreements were more extensively evaluated, by comparing individual retrievals, as a way of assessing the consistency of the crown parameters (tree height, crown width, crown height) retrieved for horizontal versus nadir scans. Tree height from the horizontal scans was obtained based on the highest and lowest return for a given point cloud. From the nadir scans, tree height was determined by the difference between a ground laser pulse return and highest top of the crown return. The inter-comparison revealed a strong correlation ($r^2 = 0.97$) with a near 1:1 relationship (Fig. 5a). The consistent findings for tree height retrievals are in part due to the capability of the experiment to acquire specific data for individual olive trees. In a complex forest environment with overlapping crowns, however, the challenge of isolating the laser pulse returns to individual trees would inhibit the ability to inter-compare structural parameter estimates, such as tree height, between horizontal and downward-viewing LiDAR data.

Similar consistent results were achieved for crown width assessments between tripod-mounted scans and nadir observations (Fig. 5b). There is a slight underestimation from the horizontal perspective, especially for larger crowns widths (>2.0 m). This underestimation could be attributed to the effect of shadowing, where the largest extents of the crown width are not captured, due to obstructing elements in the foreground. The shadowing effect does not influence the retrievals of crown width for the nadir scans, because the largest extents of the crown will be captured from the planar perspective. However, the estimates of crown height from the nadir observations will be biased due to the occlusions in the bottom part of the crown. As a result, the cross-validation of the crown heights show that there is an underestimation in E_z from nadir scans (Fig. 5c). The linear correlation is still relatively strong ($r^2 = 0.86$), but the bias in the slope of the regression indicates that crown height estimates from nadir scans must be carefully considered. The analysis of the two different perspectives of TLS data collected in this study revealed some critical findings that must be considered for future TLS-based crown structure studies. The tripod-mounted scans capture crown height E_z effectively because along the height (Z-axis), shadowing effects are minimized. However, the influence of laser pulse shadowing is captured in the range (Y-axis), thereby inhibiting an accurate estimation of the crown width. The opposite is true for the nadir perspective data, where the determination of crown width is more accurate than the retrieval of crown height, due to the confounding impact of laser pulse shadowing. Consequently, the redundancy (varying perspective) in TLS data collection for each crown illustrated the advantages and disadvantages of each viewpoint for the estimation of crown physical dimensions.

In addition to inter-comparing ILRIS-3D retrievals based on perspective, it is critical to assess the findings against traditional ground-based forest inventory measurements. Tree height estimates from the nadir and horizontal ILRIS-3D data agreed with ground measurements, with root mean square errors (rmse) of 0.43 m and 0.21 m, respectively, for a height range of 2.7–5.3 m for targeted trees (Fig. 6a). A bias in the offset of 0.28 m was observed for the nadir-based estimates. This offset could be due to the TLS detecting small leaf/branch elements at the uppermost parts of the tree crown, that are not considered in the ground-based observations with the ruler. The high spatial resolution and the close proximity of the TLS unit to the top of tree crown allow the detection of these protruding vegetative components. For the horizontal retrievals, however, this offset is not present. The horizontal

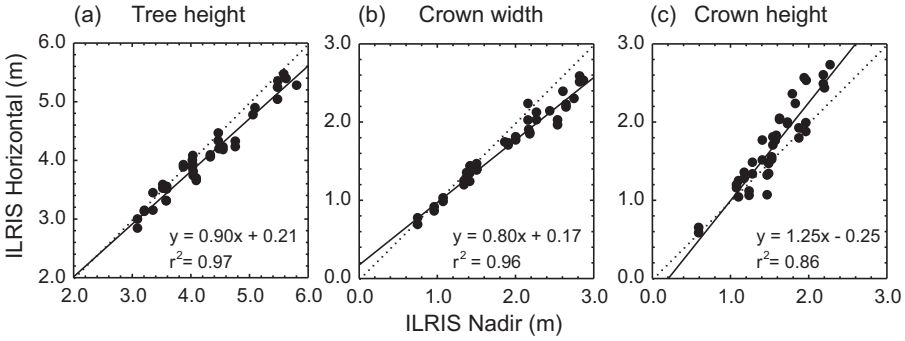

Fig. 5. Cross-validation between horizontal and nadir-based retrievals from ground LiDAR measurements yielded strong agreements for (a) tree height, (b) crown width and (c) crown height.

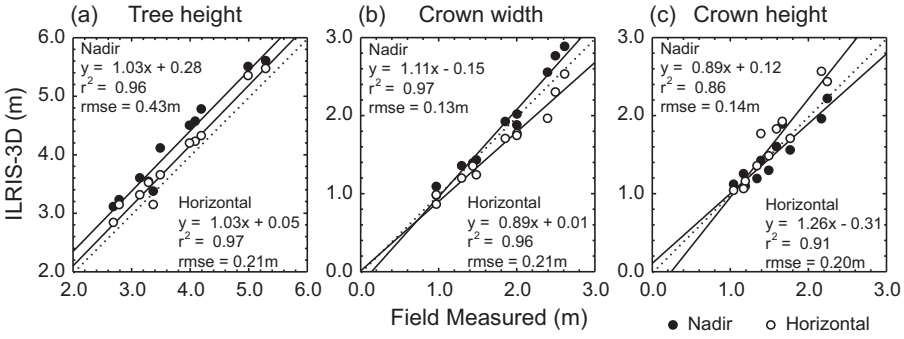

Fig. 6. High accuracies and correlations were observed when TLS-based retrievals from horizontal (open circles) and nadir (filled circles) scans were compared with ground validation metrics of (a) tree height, (b) crown width and (c) crown height.

approach mimics the perspective of the *in situ* ground methods, thereby leading to a strong agreement. Nonetheless, the cm-scale discrepancies indicate that TLS data from both tripod-mounted and nadir viewpoints are feasible methods for estimating individual tree crown height. The advantage of the TLS approach is that such tree height measurements are made much more quickly than time-consuming repetitive ground methods, and can be executed without potential systematic observer bias.

TLS-based estimates of crown width and crown height were evaluated against ground observations (Fig. 6b and c). Crown width retrievals from the TLS data strongly correlated with the validation data, with r^2 of 0.97 and 0.96 for nadir and tripod-mounted observations, respectively. Crown height assessments revealed good determination of coefficients of 0.86 and 0.91 for nadir and horizontal scans, respectively. Although not illustrated here, using merged multiple horizontal scans improved retrieval accuracies for both crown width (rmse from 0.21 to 0.12) and crown height (rmse from 0.20 to 0.11). In general, RMSE values were less than 0.21 m in all situations of crown dimension retrievals, where width ranged from 0.97 to 2.6 m and height from 1.05 to 2.25 m. As a result of the strong agreement between TLS-based estimations and ground-based measurements, the assumptions made in the slicing of the LiDAR data are considered valid for this crown type.

The TLS-based retrievals were subsequently used to calculate tree crown volumes, which were evaluated against ground-based methods. Using a technique employed in Villalobos et al. (1995), the coordinates of the tree silhouette obtained from the ground data are used to calculate tree volume. In this methodology, the projection of the tree is divided into trapezoids and the volume corresponding to each trapezoid is determined based on the second Pappus–Guldinus theorem (Villalobos et al., 1995). This process is somewhat time-consuming and can easily be replaced by TLS data. From the TLS-based definition of the shape primitives for individual crowns and the detailed profiles of crown complexity, we can obtain a detailed calculation of tree crown volume. Tree crown volume was calculated using two approaches and compared to the well-validated ground-based approach (Fig. 7). In the first approach, the E_x and E_z retrievals of the shape primitive (Fig. 3) were used to calculate the volume of the spheroid. This approximation of the spheroid volume was compared to the ground measurements and an rmse of 7.5 m^3 was determined. Although this yields a reasonable error for a tree volume range of 4.1–57.3 m^3 (Fig. 7a), a secondary technique of volume calculations was developed. The second method does not assume that the crown is a spheroid, but rather integrates the detailed TLS-profiles of the crown radius and height to estimate individual crown volume. In other words, the slicing-based approach yields not only the crown radius and crown height but also the thickness of the slice. These three values can then be used to calculate the volume of each slice and repeating this process for all subsequent slices generates a more accurate measure of total crown volume. Due to the captured detail in the TLS data, the structural complexities and variations of foliage distribution are inherently accounted for in this slice by slice-based volume calculation. The TLS-derived estimates strongly agreed with the ground-based measurements yielding an rmse of 2.6 m^3 (Fig. 7b). In this study we used a simple and efficient approach to determining crown dimensions and volume, which can replace laborious ground-based methods. Such precise and rapid retrievals of crown dimensions and volume are critical for the assessment of radiation interception and evapotranspiration, which in turn yields information about tree photosynthetic efficiency.

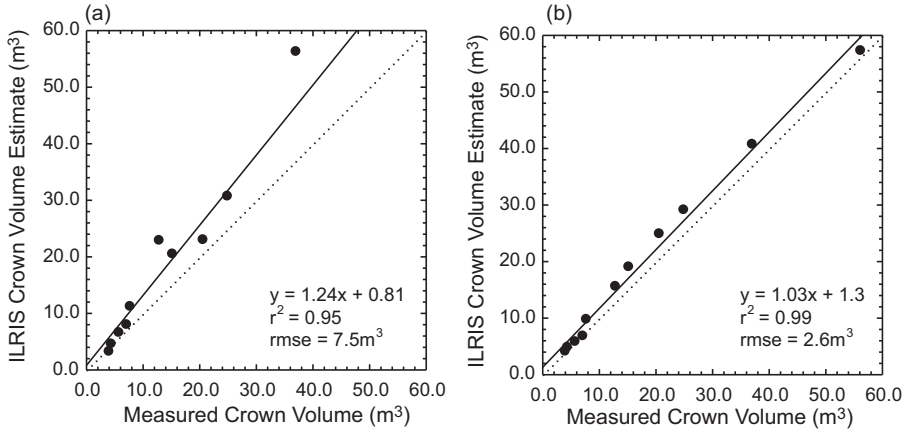

Fig. 7. Tree volume estimates from ILRIS-3D data were calculated in one case (a) using the estimated spheroid primitive and (b) integration of the crown radius profile.

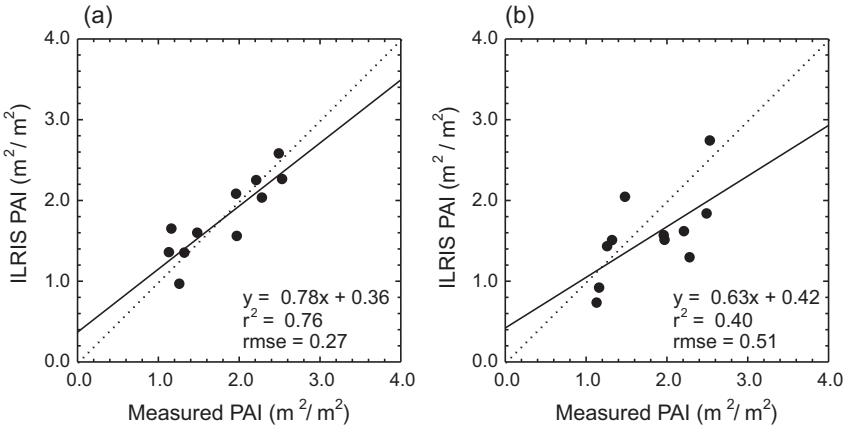

Fig. 8. Crown-level PAI retrievals from TLS data for (a) nadir and (b) horizontal perspectives. Relatively large errors of 0.27 and 0.51 m^2/m^2 were observed for a small range of 1.17–2.54 m^2/m^2.

3.2. Olive foliage assemblage properties

Crown-level PAI values were estimated from gap fraction profiles for the targeted olive trees. The approach of comparing the laser pulse return density with a theoretical maximum density provides an estimate of crown fractional cover. This value of fractional cover is inversely proportional to gap fraction, which can in turn be related to plant/leaf area index, a pertinent biological indicator of tree health condition. Appropriate acquisition and analysis of the TLS data collected in this study allows the detailed calculation of LAI at the crown-specific level. Retrievals of LAI are confounded by the influence of two factors: (a) the contribution of non-leaf material (i.e. branches, stems) and (b) the spatial organization of the foliage elements. Laboratory trials have systematically accounted for these confounding variables using an artificial tree via the calculation of the woody material index and the clumping index (Moorthy et al., 2008). In the field setting, the quantification of these parameters is more complicated. The coordinates of the laser pulse reflections do not distinguish the difference between woody and non-woody material. The intensity of the returned pulses was also carefully examined, and no systematic discernable differences between branch and foliage material were observed. The ILRIS-3D sensor is not radiometrically calibrated which thereby limited the usage of the of recorded pulse intensity as a discriminating factor. As a result, the cumulative laser pulse return density of all recorded pulses was considered a product of all tree materials made of both green and non-green components. Therefore, an alternative term, such as plant area index (PAI) is a more appropriate label for the derived indices from TLS data. Initial PAI retrievals from ILRIS-3D scans were compared to estimates from the ground-based PCA for both nadir and tripod-mounted scans (Fig. 8). PAI estimates from the nadir scans were in better agreement (rmse = 0.27) with PCA measurements as opposed to horizontal scans (rmse = 0.51), for an observed range of 1.17–2.54. The nadir observations also indicated a stronger linear agreement ($r^2 = 0.76$) versus the horizontal measures ($r^2 = 0.63$). Woody material correction from TLS data was not feasible due to the radiometrically inaccurate ILRIS-3D recorded intensities. Nonetheless, a technique was developed to determine the clumping index to account for the spatial organization of foliar elements, and its deviation from a random arrangement. Using the measured laser pulse return counts for each crown, a randomly distributed crown within the defined crown primitive was artificially simulated. Comparing the ratio of the gap fraction between the actual measured crown and the randomly organized simulated crown is an indicator of the clumping index, Ω. This index is calculated for all the olive crowns, and used as a correction factor in the retrieved PAI estimates. Assessment of the clumping-corrected PAI retrievals shows marked improvements, where rmse values improved from 0.51 to 0.26 for the horizontal scans (Fig. 9a). For the nadir scans, however, there was a marginal increase in the rmse from 0.27 to 0.28 (Fig. 9b). Both the nadir and horizontal scans revealed improved linear regression statistics when the clumping index correction was applied.

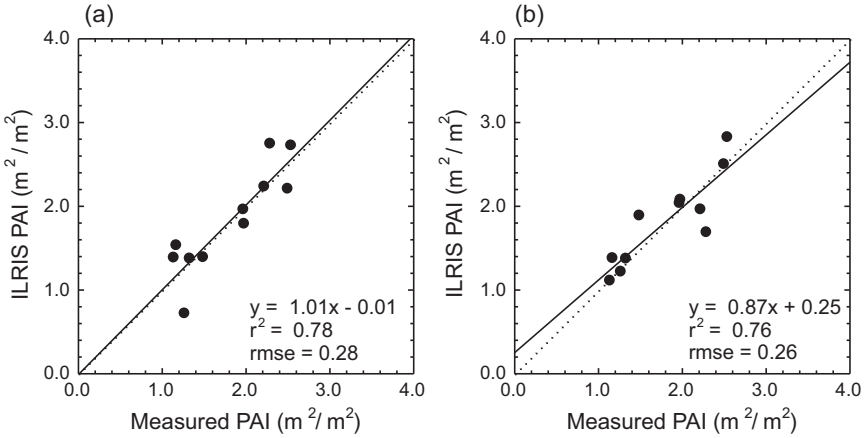

Fig. 9. The clumping index correction values improved PAI estimations for both (a) nadir and (b) tripod-mounted TLS data. Error for the horizontal scans improved from 0.51 to 0.26 m^2/m^2. Improved linear regression statistics indicate that clumping index helps to correct nadir-based PAI retrievals.

4. Conclusions

In this study we have demonstrated TLS data can be used to characterize the structural properties of individual trees provided appropriate data acquisition and analysis strategies. 24 olive tree crowns, from plantations in southern Spain, that exhibit variable structural organization, were scanned not only from a traditional tripod-mounted perspective but also from a nadir viewpoint using the ILRIS-3D. A slicing-based algorithm was developed and tested to be an efficient and effective approach for quantitative analysis and visualization of the laser pulse returns as a function of range distance, to extract dimensional variables (tree height, crown width/height, crown volume). Cross-validation between the horizontal and nadir perspectives showed consistent retrievals, with determination coefficients of 0.97, 0.96, and 0.86, for tree height, crown width and crown height, respectively. Furthermore, the TLS-based estimates were well validated with traditional *in situ* mensuration data. For crown volume cross-validation showed a determination coefficient of 0.99, with RMSE 2.6 m^3. In this study a unique approach was employed to estimate foliage assemblage parameters (crown-level gap fraction, plant area index, and clumping index) at an individual tree crown-scale unlike previous research, which often consider these factors at plot/canopy-scales. Metrics such as PAI and clumping are often integrated for a vegetation canopy and considered in 3D radiative transfer models at larger spatial scales. Plant area index estimates correlated well *in situ* measurements, when foliage clumping indices were taken into consideration (rmse of 0.28 and 0.26 for nadir and horizontal scans, respectively). The development of such robust methodologies to describe single tree crown architecture proposes the idea that perhaps TLS systems should replace current laborious and time-consuming manual approaches. It is important to note that the algorithms and techniques demonstrated here are not directly transferrable to complex forest environments. For instance, TLS data acquired in a complex, natural forest is confounded by the effect of overlapping crowns and understorey vegetation. To develop methods of robust tree crown structural parameter retrieval in such cases will first involve modification of the segmentation of the data into individual crowns, which is not a trivial process. Furthermore, understorey vegetation, if substantial enough, will cause shadowing effects that inhibit accurate crown characterization. This case of the organized plantation provides a simplified environment, but one that is worthwhile examining, for precision agriculture management. The TLS system offers a more rapid and systematic means of measuring tree crown structural properties, which are not easily obtained with traditional *in situ* methods, for agricultural monitoring and management.

Acknowledgements

The authors would like to thank the members of the Quanta Lab at the Institute for Sustainable Agriculture for their efforts during the field data collection campaign. In addition, this work was made possible with the financial support of the Natural Sciences and Engineering Research Council (NSERC) and the Canadian Foundation of Innovation (CFI).

References

Andersen, H.E., Reutebuch, S.E., McGaughey, R.J., 2006. A rigorous assessment of tree height measurements obtained using airborne lidar and conventional field methods. Canadian Journal of Remote Sensing 32 (5), 355–366.

Chen, J.M., Cihlar, J., 1995. Plant canopy gap-size analysis theory for improving optical measurements of leaf area index. Applied Optics 34 (27), 6211–6222.

Clawges, R., Vierling, L., Calhoon, M., Toomey, M., 2007. Use of a ground-based scanning lidar for estimation of biophysical properties of western larch (*Larix occidentalis*). International Journal of Remote Sensing 28 (19), 4331.

Coops, N., Wulder, M., Culvenor, D., St-Onge, B., 2004. Comparison of forest attributes extracted from fine spatial resolution multispectral and lidar data. Canadian Journal of Remote Sensing 30 (6), 855–866.

Côte, J., Widlowski, J., Fournier, R., Verstraete, M., 2009. The structural and radiative consistency of three-dimensional tree reconstructions from terrestrial lidar. Remote Sensing of Environment 113 (5), 1067–1081.

Danson, F.M., Hetherington, D., Morsdorf, F., Koetz, B., Allgower, B., 2007. Forest canopy gap fraction from terrestrial laser scanning. IEEE Geoscience and Remote Sensing Letters 4 (1), 157–160.

Donoghue, D.N.M., Watt, P.J., Cox, N.J., Wilson, J., 2007. Remote sensing of species mixtures in conifer plantations using lidar height and intensity data. Remote Sensing of Environment 110 (4), 509–522.

Harding, D., Lefsky, M., Parker, G., Blair, J., 2001. Laser altimeter canopy height profiles—methods and validation for closed-canopy, broadleaf forests. Remote Sensing of Environment 76 (3), 283–297.

Henning, J., Radtke, P., 2006. Detailed stem measurements of standing trees from ground-based scanning lidar. Forest Science 52 (1), 67–80.

Hinsley, S., Hill, R., Gaveau, D., Bellamy, P., 2002. Quantifying woodland structure and habitat quality for birds using airborne laser scanning. Functional Ecology 16 (6), 851–857.

Hopkinson, C., 2007. The influence of flying altitude, beam divergence, and pulse repetition frequency on laser pulse return intensity and canopy frequency distribution. Canadian Journal of Remote Sensing 33 (4), 312–324.

Hopkinson, C., Chasmer, L., Young-Pow, C., Treitz, P., 2004. Assessing forest metrics with a ground-based scanning lidar. Canadian Journal of Forest Research 34 (3), 573–583.

Hosoi, F., Omasa, K., 2009. Estimating vertical plant area density profile and growth parameters of a wheat canopy at different growth stages using three-dimensional portable lidar imaging. ISPRS Journal of Photogrammetry and Remote Sensing 64 (2), 151–158.

Jang, J.D., Payan, V., Viau, A.A., Devost, A., 2008. The use of airborne lidar for orchard tree inventory. International Journal of Remote Sensing 29 (6), 1767–1780.

Jupp, D.L.B., Culvenor, D.S., Lovell, J.L., Newnham, G.J., Strahler, A.H., Woodcock, C.E., 2009. Estimating forest LAI profiles and structural parameters using a ground-based laser called Echidna®. Tree Physiology 29 (2), 171–181.

Lefsky, M., Harding, D., Cohen, W., Parker, G., Shugart, H., 1999. Surface lidar remote sensing of basal area and biomass in deciduous forests of eastern Maryland, USA. Remote Sensing of Environment 67 (1), 83–98.

Lefsky, M., Cohen, W., Parker, G., Harding, D., 2002. Lidar remote sensing for ecosystem studies. Bioscience 52 (1), 19–30.

Lichti, D., Gordon, S., Stewart, M., 2002. Ground-based laser scanners: operation, systems, and applications. Geomatica 56, 21–33.

Lim, K., Treitz, P., Wulder, M., St-Onge, B., Flood, M., 2003. Lidar remote sensing of forest structure. Progress in Physical Geography 27 (1), 88–106.

Lovell, J., Jupp, D., Culvenor, D., Coops, N., 2003. Using airborne and ground-based ranging lidar to measure canopy structure in Australian forests. Canadian Journal of Remote Sensing 29 (5), 607–622.

Maas, H.G., Bienert, A., Scheller, S., Keane, E., 2008. Automatic forest inventory parameter determination from terrestrial laser scanner data. International Journal of Remote Sensing 29 (5), 1579–1593.

Means, J., Acker, S., Harding, D., Blair, J., Lefsky, M., Cohen, W., Harmon, M., McKee, W., 1999. Use of large-footprint scanning airborne lidar to estimate forest stand characteristics in the western cascades of Oregon. Remote Sensing of Environment 67 (3), 298–308.

Means, J., Acker, S., Fitt, B., Renslow, M., Emerson, L., Hendrix, C., 2000. Predicting forest stand characteristics with airborne scanning lidar. Photogrammetric Engineering and Remote Sensing 66 (11), 1367–1371.

Moorthy, I., 2009. Tree crown structural characterization: a study using terrestrial laser scanning and 3D radiative transfer modeling. PhD Dissertation. Department of Earth and Space Science, York University, Toronto, pp. 204.

Moorthy, I., Miller, J.R., Hu, B., Chen, J., Li, Q., 2008. Retrieving crown leaf area index from an individual tree using ground-based lidar data. Canadian Journal of Remote Sensing 34 (3), 320–332.

Moriana, A., Orgaz, F., 2003. Yield responses of a mature olive orchard to water deficits. Journal of American Horticultural Science 128 (3), 425–431.

Morsdorf, F., Meier, E., Kotz, B., Itten, K., Dobbertin, M., Allgower, B., 2004. Lidar-based geometric reconstruction of boreal type forest stands at single tree level for forest and wildland fire management. Remote Sensing of Environment 92 (3), 353–362.

Omasa, K., Hosoi, F., Konishi, A., 2007. 3D lidar imaging for detecting and understanding plant responses and canopy structure. Journal of Experimental Botany 58 (4), 881–898.

Pastor, M., Garía-Vila, M., Soriano, M., Vega, V., Fereres, E., 2007. Productivity of olive orchards in response to tree density. Journal of Horticultural Science and Biotechnology 82 (4), 555–562.

Patenaude, G., Hill, R., Milne, R., Gaveau, D., Briggs, B., Dawson, T., 2004. Quantifying forest above ground carbon content using lidar remote sensing. Remote Sensing of Environment 93 (3), 368–380.

Popescu, S.C., Zhao, K., 2008. A voxel-based lidar method for estimating crown base height for deciduous and pine trees. Remote Sensing of Environment 112 (3), 767–781.

Radtke, P., Bolstad, P., 2001. Laser point-quadrat sampling for estimating foliage-height profiles in broad-leaved forests. Canadian Journal of Forest Research 31 (9), 410–418.

Riaño, D., Valladares, F., Conds, S., Chuvieco, E., 2004. Estimation of leaf area index and covered ground from airborne laser scanner (lidar) in two contrasting forests. Agricultural and Forest Meteorology 124 (3–4), 269–275.

Rosell, J.R., Llorens, J., Sanz, R., Arnó, J., Ribes-Dasi, M., Masip, J., Escola, A., Camp, F., Solanelles, F., Gràcia, F., Gil, E., Val, L., Planas, S., Palacín, J., 2009. Obtaining the three-dimensional structure of tree orchards from remote 2D terrestrial lidar scanning. Agricultural and Forest Meteorology 149, 1505–1515.

Strahler, A.H., Jupp, D.L.B., Woodcock, C.E., Schaaf, C.B., Yao, T., Zhao, F., Yang, X., Lovell, J., Culvenor, D., Newnham, G., Ni-Miester, W., Boykin-Morris, W., 2008. Retrieval of forest structural parameters using a ground-based lidar instrument (ECHIDNA). Canadian Journal of Remote Sensing 34 (2), 426–440.

Suarez, L., Zarco-Tejada, P.J., Berni, J.A.J., Gonzalez-Dugo, V., Fereres, E., 2009. Modelling PRI for water stress detection using radiative transfer models. Remote Sensing of Environment 113 (4), 730–744.

Takeda, T., Oguma, H., Sano, T., Yone, Y., Fujinuma, Y., 2008. Estimating the plant area density of a japanese larch (*Larix kaempferi Sarg.*) plantation using a ground-based laser scanner. Agricultural and Forest Meteorology 148 (3), 428–438.

Thies, M., Pfeifer, N., Winterhalder, D., Gorte, B., 2004. Three-dimensional reconstruction of stems for assessment of taper, sweep and lean based on laser scanning of standing trees. Scandinavian Journal of Forest Research 19 (6), 571–581.

Thomas, V., Treitz, P., McCaughey, J., Morrison, I., 2006. Mapping stand-level forest biophysical variables for a mixedwood boreal forest using lidar: an examination of scanning density. Canadian Journal of Forest Research 36 (1), 34–47.

Villalobos, F.J., Orgaz, F., Mateos, L., 1995. Non-destructive measurement of leaf area in olive (*Olea europaea* L.) trees using a gap inversion method. Agricultural and Forest Meteorology 73 (1–2), 29–42.

Welles, J., Norman, J.M., 1991. Instrument for indirect measurement of canopy architecture. Agronomy Journal 83 (5), 818–825.

Yu, X., Hyyppa, J., Kaartinen, H., Maltamo, M., 2004. Automatic detection of harvested trees and determination of forest growth using airborne laser scanning. Remote Sensing of Environment 90 (4), 451–462.